Chemosphere 155 (2016) 292–299

Contents lists available at ScienceDirect

Chemosphere

journal homepage: www.elsevier.com/locate/chemosphere

Amitriptyline removal using palygorskite clay

Yo-Lin Tsai [a], Po-Hsiang Chang [a], Zong-You Gao [a], Xiao-Yuan Xu [a], Yan-Hsin Chen [a], Zheng-Hong Wang [a], Xin-Yu Chen [a], Zheng-Ying Yang [a], Tzu-Hao Wang [a], Jiin-Shuh Jean [a], Zhaohui Li [a, b, *], Wei-Teh Jiang [a, **]

[a] Department of Earth Sciences, National Cheng Kung University, Tainan 70101, Taiwan
[b] Geosciences Department, University of Wisconsin-Parkside, Kenosha, WI 53141-2000, USA

HIGHLIGHTS

- Palygorskite (PFl-1) is effective for the removal of amitriptyline (AMI).
- Uptake of AMI on PFl-1 is restricted to the external surfaces with fast rate.
- Cation exchange was the dominant mechanism for AMI uptake on PFl-1.
- Minor component smectite in PFl-1 contributed significantly to AMI uptake.

ARTICLE INFO

Article history:
Received 23 December 2015
Received in revised form
1 April 2016
Accepted 18 April 2016

Handling Editor: Shane Snyder

Keywords:
Amitriptyline
Cation exchange
Palygorskite clay
Mechanism
Removal
Uptake

ABSTRACT

With the increased detections of commonly used pharmaceuticals in surface water and wastewater, extensive attentions were paid recently to the fate and transport of these pharmaceuticals in the environment. Amitriptyline (AMI) is a tricyclic antidepressant widely applied to treat patients with anxiety and depression. In this study, the removal of AMI with palygorskite clay (PFl-1) was investigated under different physico-chemical conditions and supplemented by instrumental analyses. The uptake of AMI on PFl-1 was well fitted by the Langmuir isotherm with an adsorption capacity of 0.168 mmol g^{-1} at pH 6–7. The AMI uptake was fast and reached equilibrium in 15 min. The X-ray diffraction patterns showed no shift of the (110) peak position of palygorskite after AMI uptake. However, the (001) peak position of the minor component smectite (about 10%) shifted to lower angle as the amounts of AMI input increased. These results suggested surface uptake of AMI on palygorskite and interlayer uptake of AMI in smectite. As smectite is a common component of palygorskite clays, its role in assessing the properties and performances of palygorskite clays for the uptake and removal of contaminants should not be neglected. Overall, the high affinity of AMI for PFl-1 and strong retention of AMI on PFl-1 suggested that it could be a good adsorbent to remove AMI from wastewater. Palygorskite clays can also be a sink for many cationic pharmaceuticals in the environmental of the arid regions.

1. Introduction

Amitriptyline (AMI) is a tricyclic antidepressant widely applied to treat patients with anxiety and depression (Lee et al., 2005). Just in England alone, the annual consumption of AMI was 5.9 metric tons in 2000 (Sebastine and Wakeman, 2003). The extensive use of AMI and its persistence in ambient temperature resulted in its frequent detection in wastewater, surface runoff, and effluents from sewage treatment plants (Li et al., 2013) with concentrations in the ranges of 0.5–21 ng l^{-1} (Calisto and Esteves, 2009). Although about 98% AMI removal could be achieved using a membrane bioreactor (Tadkaew et al., 2011), it was listed as non-biodegradable (Richardson and Bowran, 1985) and a 100% detection of AMI was still reported at the effluent of Cilfynydd wastewater treatment plant after treatment (Kasprzyk-Hordern et al., 2009). In addition, there was a considerable lack of knowledge about the environmental fate of a large number of psychiatric pharmaceuticals, including AMI, and further research about this topic was in great

* Corresponding author. Geosciences Department, University of Wisconsin-Parkside, Kenosha, WI 53141-2000, USA.
** Corresponding author. Department of Earth Sciences, National Cheng Kung University, Tainan 70101, Taiwan
E-mail addresses: li@uwp.edu (Z. Li), atwtj@mail.ncku.edu.tw (W.-T. Jiang).

http://dx.doi.org/10.1016/j.chemosphere.2016.04.062
0045-6535/

need (Calisto and Esteves, 2009). Moreover, as their persistence and accumulation in the environment were very likely to occur, additional high quality sorption data for structurally diverse compounds, specifically ionic compounds, would be needed for the development of robust assessment techniques used in complex systems such as sewage sludge (Stevens-Garmon et al., 2011; Hörsing et al., 2011; Hyland et al., 2012).

Clay minerals have large surface areas and high cation exchange capacities and thus are commonly studied for their sorptive removal of contaminants. Interactions between AMI and clay minerals were focused on montmorillonite and kaolinite, as these are the common soil minerals found in most regions (Lv et al., 2013; Chang et al., 2014). In comparison to these platy clay minerals, palygorskite is a magnesium-aluminum phyllosilicate with a fibrous form. It has been commonly found in soils and sediments of arid regions and is often used in antidiarrheal medications. It is estimated that 1,300,000 tons were produced annually with the United States as the largest producer (Murray et al., 2011). Because of periodic reversal of the tetrahedral sheets (every two tetrahedra for palygorskite and every three tetrahedra for sepiolite), it has a periodic array of octahedral ribbons and forms a chain-like structure parallel to the fiber stretch (Galan, 1996). The space inside each channel is large enough to accommodate exchangeable cations and water molecules. As an adsorbent, most studies on palygorskite were conducted for the removal of heavy metals and dyes (Galan, 1996; Sanchez et al., 1999; Taha et al., 2013).

The chain-like structure rendered its expandability, thus, restricted the entrance of larger organic cations into the channels. For this reason, it is anticipated that its behavior for the uptake of cationic drugs would be different from other platy clay minerals and be different from its uptake of small inorganic cations as well. As smectite is a common component in palygorskite clays (Galan, 1996), an evaluation of the possible contribution of smectite component to the adsorption of cationic drugs onto palygorskite clays is particularly of great interest. The goal of this research was to study the interactions between AMI and palygorskite in order to decipher the mechanisms of AMI removal by palygorskite, and to contrast the differences in the uptake of cationic drugs between fibrous clay minerals and platy clay minerals, so that its use in wastewater treatment could be extended.

2. Materials and methods

2.1. Materials

The AMI used was in an HCl form with a molecular weight of 313.9 g mol^{-1} and a pK_a value of 9.4 (Green, 1967) or 9.45 (Manzo et al., 2006) (Fig. 1a). It is freely soluble in water, while its basic form was virtually insoluble in water (Manzo et al., 2006). It was purchased from Sigma–Aldrich, USA. The PFl-1 palygorskite clay was obtained from the Source Clay Minerals Repository. It contained ~80% palygorskite, 10% smectite, 7% quartz, 2% feldspar, and 1% other (Chipera and Bish, 2001). It had a reported cation exchange capacity (CEC) of 0.175 $mmol_c\ g^{-1}$ (Borden and Giese, 2001) and a specific surface area (SSA) of 173 $m^2\ g^{-1}$ (Dogan et al., 2006).

As the sample contained 10% smectite and it was difficult to find pure palygorskite, to evaluate the relative contribution of palygorskite and smectite in PFl-1, a sepiolite (SepSp-1) acquired from the Source Clay Minerals Repository was used as a replacement for pure palygorskite to test its adsorption capacity of AMI. X-ray diffraction analyses identified sepiolite as the only mineral phase (Gehring et al., 1995). It has a reported CEC of 0.17 $mmol_c\ g^{-1}$, similar to that of the PFl-1 (Table 1), and an SSA of 317 $m^2\ g^{-1}$ (Jaynes et al., 2005).

2.2. Batch AMI adsorption experiments

To each 50 mL centrifuge tube, 0.1 g of palygorskite clay and 20 mL AMI solution at concentrations of 0.16–1.91 mM were combined for the isotherm experiment. An initial concentration of 1.59 mg L^{-1} was used for studies conducted under different contact times, solution pHs, ionic strengths, and temperatures. The mixtures were shaken on a reciprocal shaker at 150 rpm at room temperature for 24 h, except the kinetic study. The centrifuge tubes were wrapped with aluminum foils to prevent possible photodegradation of AMI. After mixing, samples were centrifuged at 8000 rpm for 10 min and the supernatants were passed through 0.22 μm filters before being analyzed for equilibrium AMI concentrations by a UV–Vis method. For the kinetic study, the mixtures were shaken for 0.25, 0.5, 1.0, 2.0, 4.0, 8.0, 16, and 24 h. For the pH adsorption edge experiment, the equilibrium solution pH varied between 2 and 11 and was adjusted by adding minute amounts of 2 M NaOH or 2 M HCl gradually and checked every 6 h. For the ionic strength experiment, NaCl was used as the ionic strength adjuster with concentrations of 0.001, 0.01, 0.1, and 1.0 M. For temperature effect study, the temperature was maintained at 303, 313, and 323 K. All experiments were conducted in duplicate.

2.3. Methods of analysis

The AMI concentration was measured using a UV–Vis spectrophotometer (SmartSpec 3000, Bio-Rad Corp.) at the detection wavelength of 240 nm with a detection limit of 0.3 mg L^{-1} and a linear response range of 1–125 mg L^{-1}. Under the experimental conditions AMI existed as a cation and cation exchange may play a significant role in AMI uptake. Thus, the amounts of Na^+, K^+, Mg^{2+}, and Ca^{2+} released from PFl-1 were analyzed by ion chromatography (IC) (Dionex 100) with a mobile phase made of 20 mM methanesulfonic acid. The equilibrium concentrations were in the respective ranges of 0.03–0.05, 0.01–0.03, 0.03–0.18, and 0.18–0.51 mM for Na^+, K^+, Mg^{2+}, and Ca^{2+} desorption under different initial AMI concentrations.

The FTIR spectra were acquired on a Jasco FT/IR-4100 spectrometer equipped with a ZnSe attenuated total reflection accessory. The spectra were acquired from 600 to 4000 cm^{-1} by accumulating 256 scans at a resolution of 4 cm^{-1}. Powder XRD analyses were performed on a Bruker D8 Advance diffractometer utilizing CuKα radiation at 30 kV and 40 mA and samples were scanned from 2° to 26° 2 θ at 1°min^{-1} with a scanning step of 0.02°. For SEM observation, PFl-1 powder taken from a blank sample was dried at room temperature and coated with Pt. An FEI Quanta 250 FEG SEM operated at an accelerating voltage of 7 kV was used.

3. Results and discussion

3.1. Influence of initial concentration on AMI removal

The data of AMI uptake on PFl-1 under different initial concentrations at pH = 6–7 were fitted using the Langmuir and Freundlich adsorption models and the former fitted to the experimental data better (Fig. 1b). The Langmuir model assumed monolayer adsorption on the absorbent with limited capacity, while the Frenudlich model could be used for heterogeneous multilayer adsorption (Banu et al., 2015). The Langmuir model can be described as:

$$C_S = \frac{K_L C_m C_L}{1 + K_L C_L} \quad (1)$$

where C_S is the amount of AMI adsorbed on solid at equilibrium

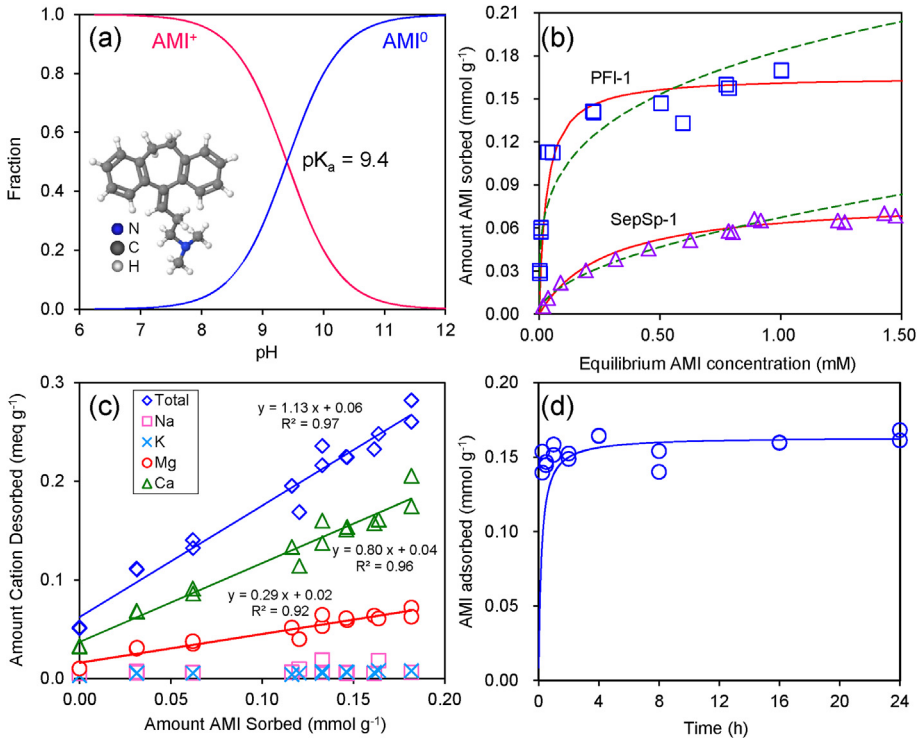

Fig. 1. Speciation of AMI under different pH conditions (a). Uptake of AMI on PFI-1 and SepSp-1 (b), release of exchangeable cations accompanying AMI uptake on PFI-1 (c), and fitting of pseudo-second-order kinetic model to the kinetic data of AMI removal by PFI-1 (d) at pH 6–7. The solid and dash lines in (b) are the Langmuir and Freundlich fits to the experimental data.

(mmol g^{-1}), C_L is the equilibrium solute concentration (mM), K_L is the Langmuir coefficient (L $mmol^{-1}$), and C_m is the adsorption capacity (mmol g^{-1}). While for the Freundlich model, it is expressed as:

$$C_S = K_F C_L^{1/n} \quad (2)$$

where K_F is the Freundlich adsorption coefficient. The r^2 value was 0.988 and 0.899 when the Langmuir and Freundlich models were used to fit the experimental data. The K_F value was 12.9 L kg^{-1} and the n value was 0.24 based on the Freundlich fit. The AMI adsorption capacity on PFI-1 was 0.168 mmol g^{-1}. This value agrees well with the CEC value of 0.175 meq g^{-1} (Borden and Giese, 2001). In comparison, the adsorption capacity of AMI on Ca-montmorillonite (SAz-2) and kaolinite (KGa-2) was 1.05 and 0.015 mmol g^{-1}, respectively (Table 1), also agreeing well with their CEC values (Lv et al., 2013; Chang et al., 2014). Moreover, the uptake capacity of ranitidine, a cationic drug with a p*K*a value of 8.2, on PFI-1 was 0.156 mmol g^{-1}, slightly less than the CEC of PFI-1 (Li et al., 2016). The results showed that CEC was the dominant factor in AMI uptake on clay minerals regardless whether they are in platy or in fibrous forms and the uptake of AMI on PFI-1 was via a cation exchange mechanism.

The AMI uptake on sepiolite resulted in a capacity of 0.080 $mmol_c$ g^{-1}, about half of its CEC value (Fig. 1b). Both palygorskite and sepiolite are fibrous clay minerals with their channel sizes of 3.7 × 6.4 Å for palygorskite and 3.7 × 10.6 Å for sepiolite (Galan, 1996) and parts of the cation exchange sites were in the channels. The computed molecular size of AMI was 10.68 Å × 8.57 Å × 5.89 Å (Bindya et al., 2007). The larger molecular size of AMI may restrict its entrance into the channels, resulting in surface uptake of AMI limited on the external surfaces. This could account for the much lower AMI uptake capacity in comparison to the CEC value of the mineral (Table 1). As such, much of the AMI uptake on PFI-1 could be attributed to the uptake by the minor component smectite.

The IC results showed that Ca^{2+} and Mg^{2+} were the major elements released and the release of K^+ and Na^+ was low and almost constant during the AMI adsorption. The desorption of metal cations showed a positive linear correlation with the amount of AMI adsorbed with a slope of 1.1 (Fig. 1c). The near unit slope further confirmed that the cation exchange mechanism of AMI uptake on PFI-1, similar to an observation with a slope of 1.2 for AMI uptake on smectite (Chang et al., 2014).

3.2. Kinetics of AMI removal

AMI removal by PFI-1 was fast and equilibrium was reached in a few minutes of mixing (Fig. 1d). The pseudo-second-order kinetic model fitted well to the experimental data. The model was used to describe chemisorption and has been widely applied to the adsorption of pollutants from aqueous solutions based on the following equation (Blanchard et al., 1984):

$$q_t = \frac{kq_e^2 t}{1 + kq_e t} \quad (3)$$

where q_t (mmol g^{-1}) is the amount of AMI adsorbed on the surface of the adsorbent in time t, k (g $mmol^{-1}$ h^{-1}) is the rate constant of adsorption, and q_e (mmol g^{-1}) is the amount of AMI adsorbed at equilibrium. Eq. (3) can be rearranged to a linear form of

$$\frac{t}{q_t} = \frac{1}{kq_e^2} + \frac{1}{q_e} t \quad (4)$$

where kq_e^2 is the initial rate (mmol g^{-1} h^{-1}). The fitted rate constant

Table 1
Physical and chemical properties of PFl-1, SepSp-1, SAz-2, and KGa-2 clays.

	Bulk PFl-1 clay	Calculated pure palygorskite	SepSp-1 sepiolite	SAz-1 smectite	KGa-2 kaolinite
Cation exchange capacity (meq 100^{-1} g^{-1})	17.5[a]	5.5 (calculated)[b]	17[c]	123[a]	3.7[a]
Main exchangeable cation	Ca, Mg[b]	–	Ca, Na[d]	Ca[e]	Na[f]
Surface area (m^2 g^{-1})	173[g]	–	317[c]	65[g]	21.7[g]
AMI Langmuir adsorption capacity (mmol g^{-1})	0.168[b]	0.056 (calculated)[b]	0.080[b]	1.05[e]	0.015[f]
Mineral constituents	~80% palygorskite, 10% smectite, 7% quartz, 2% feldspar, 1% other[h]	100% palygorskite (normalized)	95–100% sepiolite, <2% quartz[d]	~99% smectite, 1% other[h]	~96% kaolinite, 3% anatase, 1% crandallite, mica or illite[h]
Chemical composition (in weight)	60.9% SiO_2, 10.4% Al_2O_3, 0.49% TiO_2, 2.98% Fe_2O_3, 0.40% FeO, 0.058% MnO, 10.2% MgO, 1.98% CaO, 0.058% Na_2O, 0.80% K_2O, 0.542% F, 0.80% P_2O_5, 0.11% S[i]	–	52.9% SiO_2, 2.56% Al_2O_3, <0.001% TiO_2, 1.22% Fe_2O_3, 0.3% FeO, 0.13% MnO, 23.6% MgO, 0.01% CaO, 0.01% Na_2O, 0.05% K_2O, 0.01% P_2O_5, 20.8% LOI[d]	60.4% SiO_2, 17.6% Al_2O_3, 0.24% TiO_2, 1.42% Fe_2O_3, 0.08% FeO, 0.099% MnO, 6.46% MgO, 2.82% CaO, 0.063% Na_2O, 0.19% K_2O, 0.287% F, 0.02% P_2O_5[i]	43.9% SiO_2, 38.5% Al_2O_3, 2.08% TiO_2, 0.98% Fe_2O_3, 0.15% FeO, 0.03% MgO, 0.005% Na_2O, 0.065% K_2O, 0.02% S, 0.045% P_2O_5[i]

[a] Borden and Giese, 2001.
[b] This study.
[c] Jaynes et al., 2005.
[d] Clay minerals society source clays repository (http://www.clays.org/SOURCE%20CLAYS/SCdata.html).
[e] Chang et al., 2014.
[f] Li et al., 2013.
[g] Dogan et al., 2006.
[h] Chipera and Bish, 2001.
[i] Ahmet and Angel, 2001.

was 33.9 g $mmol^{-1}$ h^{-1} with a q_e value of 0.163 mmol g^{-1}. The rate constant of AMI uptake on PFl-1 was nearly twice to that of value of 18.2 g $mmol^{-1}$ h^{-1} for AMI uptake on SAz-2 (Chang et al., 2014). The fast uptake of AMI on PFl-1 again suggested that the uptake of AMI was limited to the external surfaces of PFl-1. Similarly, the uptake of ranitidine on PFl-1 was also instantaneous (Li et al., 2016). The fast AMI uptake indicated PFl-1 is practically feasible to be used as adsorbents for the removal of cationic drugs.

3.3. Influence of solution pH and ionic strength

The speciation of AMI was different under different pH conditions (Fig. 1a). When the equilibrium solution pH was below the pK_a value, the amine group of AMI became protonated, resulting in a positively charged AMI^+. In this case, the difference among the uptake of AMI on PFl-1 was minimal (Fig. 2a). In contrast, when the solution pH was greater than the pK_a value, apparent AMI removal increased significantly, up to about 0.32 mmol g^{-1} at pH 11. The equilibrium AMI concentrations were 0.018–0.024 mM at pH 9 to 11. It was speculated that the solubility of AMI might decrease significantly when the solution pH was greater than its pK_a. Tests on AMI solubility as a function of pH showed a solubility of only 0.035 and 0.025 mM at pH 10 and 11, respectively (Fig. 2b). Thus, the extremely high apparent AMI removal from water at high solution pH was caused by the decreased solubility of AMI, resulting in precipitation of AMI instead of adsorption. However, no separate AMI phase was identified in the XRD patterns (see section 3.5). This would be attributed to amorphous AMI precipitation or minute amounts of AMI that cannot be detected by XRD analyses. Similarly, an extremely high uptake of AMI was also found on SAz-2 at high pH but the consequences were not explained in the original study (Chang et al., 2014). It could be due to the same effect of AMI precipitation at pH 9–10, too.

As the solution NaCl concentration increased from 0.001 to 1.0 M, the removal of AMI by PFl-1 increased from 0.18 to 0.20 mmol g^{-1} (Fig. 2c). This minute increase in AMI uptake may suggest that Na^+ had minimal competition against AMI for the adsorption sites on PFl-1. In comparison, a slight decrease in AMI uptake on SAz-2 was found as the NaCl concentration increased from 0.1 mM to 1 M (Chang et al., 2014). Moderate decrease in AMI uptake on KGa-2 was found as the ionic strength increased (Lv et al., 2013). The result implied that the AMI adsorption onto palygorskite formed a strong surface interaction as compared with that between AMI and smectite or kaolinite. Such an implication is further evidenced by the FTIR result below.

3.4. Effect of experimental temperature

At the initial AMI concentration of 1.59 mM, AMI uptake increased as the temperature increased (Fig. 2d), suggesting an endothermic adsorption process. The thermodynamic parameters of AMI adsorption are related to the AMI partitioning coefficient by:

$$\ln K_d = -\frac{\Delta H}{RT} + \frac{\Delta S}{R} \quad (5)$$

where ΔH is the change of enthalpy after adsorption, T is the temperature in K, R is the gas constant, ΔS is the change in entropy, and K_d is the ratio of AMI concentration in the adsorbent to that in solution. The free energy of adsorption ΔG is linked to these thermodynamic parameters by:

$$\Delta G = \Delta H - T\Delta S \quad (6)$$

The calculated ΔG, ΔH, and ΔS values were −11 to −12 kJ mol^{-1}, 10 kJ mol^{-1}, and 0.07 kJ mol^{-1} K^{-1}, respectively, in comparison to −9 to −11 kJ mol^{-1}, 11 kJ mol^{-1}, and 0.07 kJ $(mol\text{-}K)^{-1}$ for AMI uptake on KGa-2 (Lv et al., 2013). The small negative ΔG values suggested physical adsorption such as cation exchange as observed in AMI uptake on KGa-2 and SAz-2 (Lv et al., 2013; Chang et al., 2014). In addition, for the same PFl-1, the uptake of tetracycline and ranitidine resulted in ΔG values of −11 to −28 kJ mol^{-1} (Chang et al., 2009) and −13 to −15 kJ mol^{-1} (Li et al., 2016). As all these drugs are in cationic forms in the tested pH range, the similar ΔG values of their sorption on PFl-1 suggested similar dominant mechanism of their uptake, i.e. a cation exchange mechanism. Based on the aforementioned comparable parameters, AMI adsorption onto the predominant constituent of PFl-1, palygorskite was likely to have similar thermodynamic properties and follow

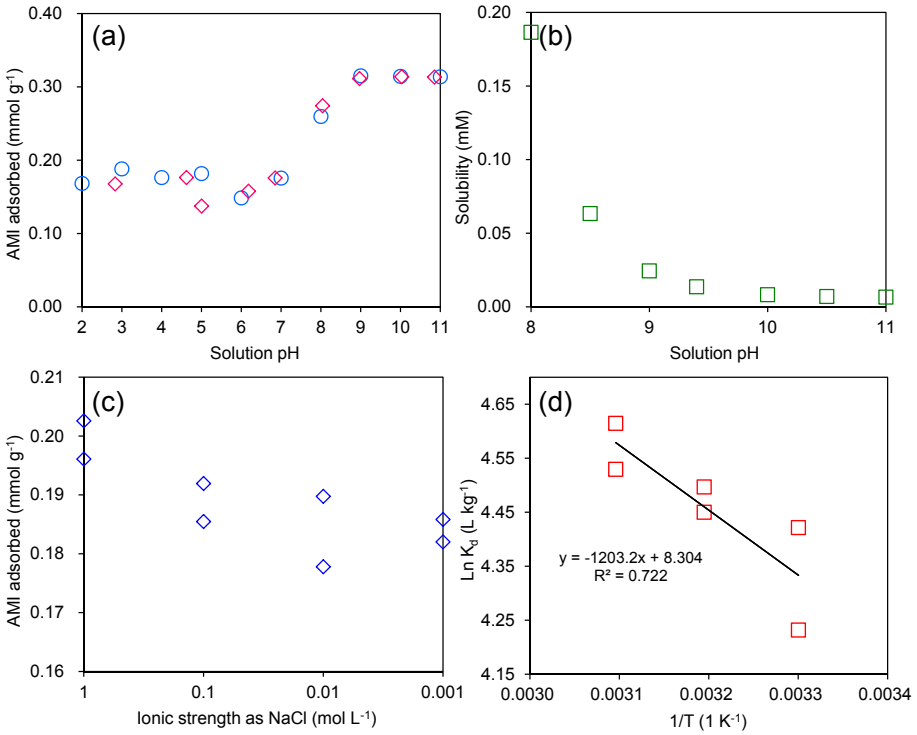

Fig. 2. Uptake of AMI on PFl-1 as affected by equilibrium solution pH (a), solubility of AMI in aqueous solution at different pH (b), and AMI uptake on PFl-1 as affected by ionic strength (c) and temperature (d) at pH 6–7.

the same mechanism as that by the minor component smectite, although the smectite made a significant impact to the AMI adsorption capacity of PFl-1.

3.5. FTIR and XRD analysis

The FTIR spectra of raw AMI, AMI-adsorbed PFl-1 under different initial concentrations, and AMI mechanically mixed with PFl-1 at 0.16 mmol g^{-1} were plotted in Fig. 3. The bands at 1472 and 1344 cm^{-1} were due to the N–CH_3 stretching, whereas the bands at 1600, 1580, 1500, and 1450 cm^{-1} were due to the aromatic groups (Vijaya et al., 2015). The 2949 and 2825 cm^{-1} were assigned to the asymmetric and symmetric CH_3 stretching vibration while those at 2921 and 2852 cm^{-1} were assigned to the asymmetric and symmetric CH_2 stretching vibration (Blessel et al., 1974). The significant changes in the spectra of the samples were observed in the region of 700–800 cm^{-1}. The absorption bands of AMI at 750 and 767 cm^{-1} were attributed to four adjacent hydrogen atoms on the benzene ring (Blessel et al., 1974), which shifted to higher frequencies after AMI uptake on the PFl-1 surfaces. The characteristic bands of Si–O stretching at 978, 1019, and 1194 cm^{-1} for PFl-1 (Madejova and Komadel, 2001) showed obvious shift after AMI uptake, implying strong interactions between the protonated AMI molecules and the broken Si–O–Si bonds at the edges of the structural channels at the external surface of palygorskite. Such changes of Si–O stretching bands were not reported for the AMI uptake by smectite in which AMI adsorption was dominated by interlayer intercalation (Chang et al., 2014). Smectite has broken Si–O–Si bonds only at the edges or defective sites of silicate layers.

The XRD patterns of raw PFl-1, raw AMI, and AMI-adsorbed PFl-1 under different initial concentrations were plotted in Fig. 4a. The most characteristic peak of palygorskite is the (110) reflection located at 8.4° 2 θ. This peak showed no shift after uptake of different amounts of AMI. The peak at 5.73° 2 θ prior to AMI adsorption was due to the (001) reflection of smectite. Its d-spacing was 15.4 Å, suggesting that the minor smectite component was in the calcium form. This observation agreed well with the Ca^{2+}

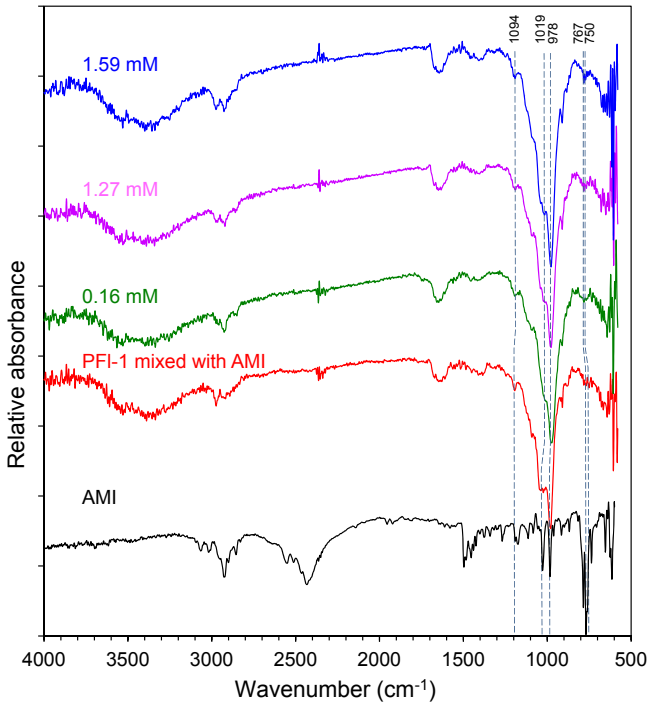

Fig. 3. FTIR spectra of crystalline AMI, AMI adsorbed on PFl-1 under three different initial concentrations at pH 6–7, and AMI mechanically mixed with PFl-1 at 0.16 mmol g^{-1}. Vertical dash lines indicate shifting of the absorption bands characteristic of AMI at 750 and 767 cm^{-1} and palygorskite at 978, 1019, and 1194 cm^{-1}.

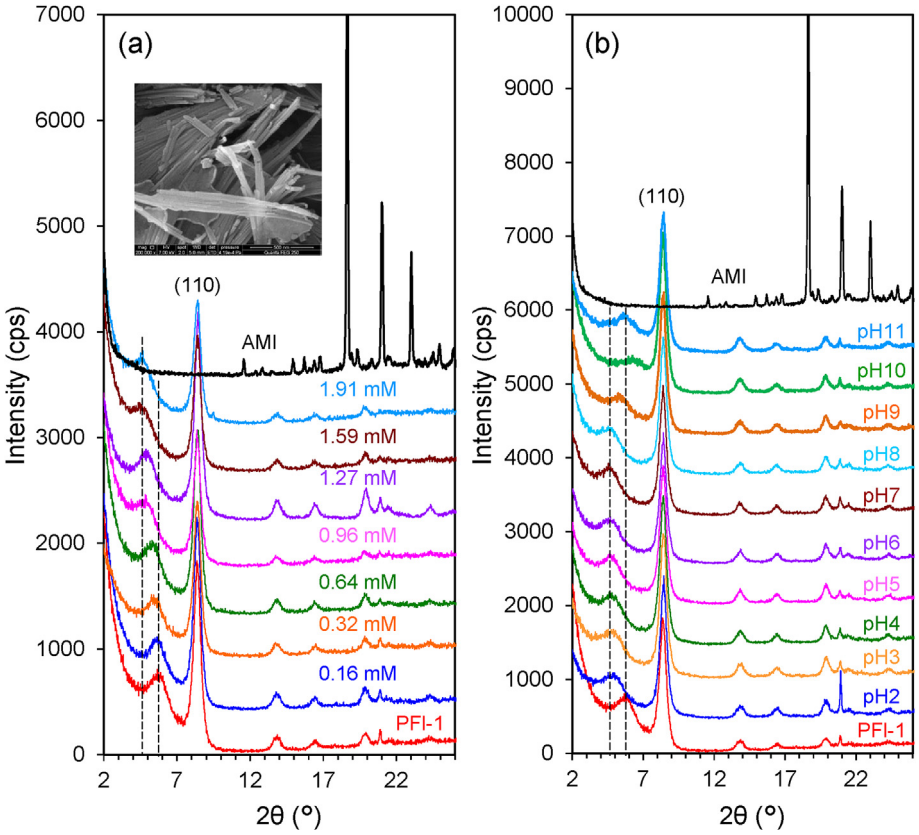

Fig. 4. X-ray diffraction patterns of raw PFl-1, crystalline AMI, and AMI adsorbed on PFl-1 at different initial AMI concentrations at pH 6–7 (a) and at different pH values with an initial AMI concentration of 1.59 mM (b). The dashed lines indicated the (001) reflection of montmorillonite present in the PFl-1 sample. Its d-spacing increased as the amount of AMI uptake increased (a) and decreased when solution pH was 9 and above (b). The inset is a SEM image of palygorskite fibers and curvy smectite flakes in PFl-1 (ca. 1.5 μm in width).

desorption data in the IC study. Meanwhile, as the amounts of AMI uptake increased, the (001) reflection of smectite shifted towards the low angle and the d_{001} value increased, suggesting progressive interlayer uptake of AMI. The XRD patterns of AMI-adsorbed PFl-1 as affected by solution pH were shown in Fig. 4b. The d_{001}-spacing of smectite component remained the same at pH 2–8, reconfirming the almost identical AMI uptake in this pH range (Fig. 2a). The reduction in d_{001}-spacing of smectite at pH 9–11 reflected a reduced uptake of AMI at high pH, confirming our previous speculation that the apparently high removal of AMI from solution at pH 9–11 was via precipitation instead of adsorption. Due to the lack of AMI peaks in these XRD patterns, the AMI precipitation was most likely in an amorphous form.

3.6. Discussion

The channel size is 3.7 Å × 6.4 Å and 3.7 Å × 10.6 Å for palygorskite and sepiolite, respectively (Galan, 1996), while the computed molecular size of AMI was 10.68 Å × 8.57 Å × 5.89 Å (Bindya et al., 2007). Thus, the channel size of palygorskite or sepiolite is too small to accommodate AMI. In such a case, the adsorbed AMI can only be retained on the external surface of palygorskite. Molecular simulations showed that AMI adopted both folded and extended side-chain conformations (Heimstad et al., 1991). However, the ribbon-like structure of palygorskite may create an ideal site for AMI uptake (Fig. 5). Using the AMI adsorption capacity of 0.168 mmol g^{-1} and the SSA of 173 m^2 g^{-1} (Dogan et al., 2006), the calculated area per AMI molecule is 171 $Å^2$, agreeing well with the minimal surface area of AMI occupied at the air–water interface at about 170 $Å^2$ (Taboada et al., 2001). The close match between these values suggested a monolayer AMI surface coverage with respect to the PFl-1 surfaces, confirming the validity of using the Langmuir isotherm to fit the experimental data. In comparison, for kaolinite, the calculated surface area occupied per AMI molecule was 260–270 $Å^2$ (Lv et al., 2013).

The PFl-1 is made of ~80% palygorskite, 10% smectite, 7% quartz, 2% feldspar, and 1% other (Chipera and Bish, 2001). It contains a significant amount of Ca (Ahmet and Angel, 2001) and its major exchangeable cations were shown to be Mg^{2+} and Ca^{2+} (Fig. 1c), in good agreement with Ca-montmorillonite as the minor smectite component of PFl-1. The CEC of PFl-1 was 0.175 meq g^{-1} (Borden and Giese, 2001). For Ca-montmorillonite SAz-1, its CEC is 1.2 meq g^{-1} (Table 1). At 10% smectite, the contribution of smectite to the total CEC of PFl-1 would be 0.12 meq g^{-1}. The remaining CEC of 0.055 meq g^{-1} would be originated for palygorskite. Thus, since cation exchange was considered as the most important mechanism of AMI adsorption on palygorskite, at the AMI adsorption capacity, the 10% smectite contributed to two-thirds of AMI removal, while the 80% palygorskite contributed to only one-third of the total AMI uptake of 0.168 mmol g^{-1}. The CEC of palygorskite clays range from 0.04 to 0.4 meq g^{-1} and are typically in the range of 0.2–0.3 meq g^{-1}, but the larger values are likely related to impurities, particularly smectite (Galan, 1996; Shuali et al., 2011). The smaller CEC values like 0.076 meq g^{-1} reported for the palygorskite from Quincy, Florida (Shuali et al., 2011) had the same order of magnitude as the calculated CEC for the palygorskite in PFl-1 clay in this study.

Thus, the AMI adsorption on the palygorskite alone in PFl-1

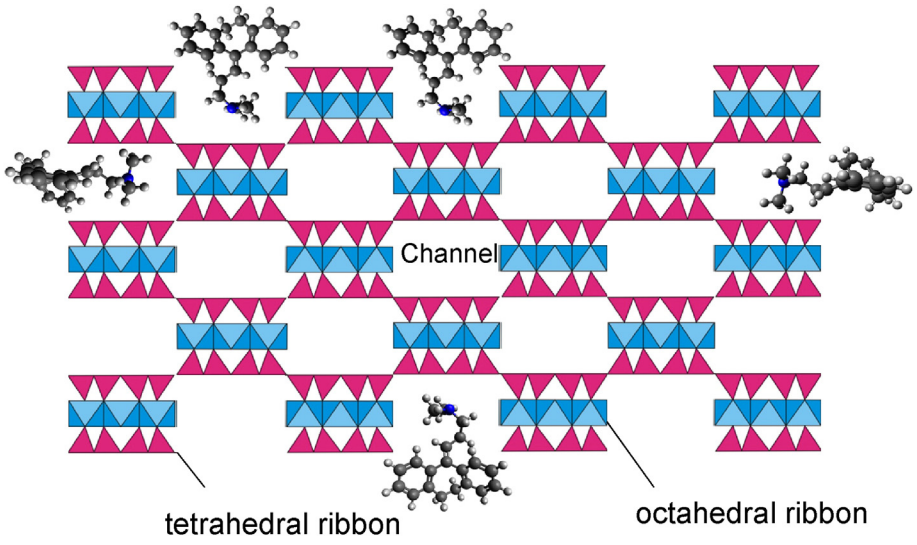

Fig. 5. Illustration of uptake of AMI on PFl-1 surfaces via the ribbon-like structure.

could reach a capacity of 0.056 mmol g^{-1} with a fast adsorption rate and relatively strong interaction through a cation exchange mechanism on the external surface. Based on the same approach, the close match of the adsorption of AMI, ranitidine, ciprofloxacin, or tetracycline cations onto PFl-1 (Chang et al., 2009; Chang et al., 2016; Li et al., 2016) and the CEC value of PFl-1 in near neutral solution would imply similar influences and interactions in all these adsorption processes. The determination of adsorption mechanism in neutral solution does not seem to be affected by the presence of minor smectite, although the contribution of smectite (when present) to the CEC of palygorskite clays, and therefore, to the uptake of organic cations should not be neglected. The adsorption conformable to CEC also indicates that PFl-1 or other palygorskite clays could be an effective adsorbent for the removal of cationic drugs in wastewater treatment.

Researches on effective removal of emerging pharmaceuticals are still in great need (Calisto and Esteves, 2009) and conflicting results were reported in the literature. For examples, AMI can be readily oxidized by permanganate under the acidic environment (Lamani and Nandibewoor, 2011), but not biodegradable under sewage treatment conditions (Richardson and Bowran, 1985). In a membrane bioreactor about 98% AMI removal was reported (Tadkaew et al., 2011). Considerable amounts of AMI removal were found using activated sludge with high CEC values (Hyland et al., 2012). However, a 100% detection of AMI was found at the effluent of Cilfynydd wastewater treatment plant after treatment (Kasprzyk-Hordern et al., 2009). Activated carbon (AC) was studied for the adsorptive removal of AMI with capacities at 0.2–0.3 mmol g^{-1} (Ledesma et al., 2010) and 0.1–0.3 mmol g^{-1} (Nabais et al., 2012). The AMI adsorption capacity on PFl-1 at 0.168 mmol g^{-1} is comparable to that on AC, but the cost of palygorskite clay would be much cheaper than AC, making it a possible candidate as adsorptive agents for the removal of cationic drugs in wastewater treatment.

4. Conclusions

The removal of AMI by PFl-1 showed a pseudo-second-order kinetics with a rate constant of 33.9 g $mmol^{-1}$ h^{-1} and followed the Langmuir isotherm with a capacity of 0.168 mmol g^{-1}, agreeing well with the CEC values of the PFl-1. The influence of ionic strength and temperature on AMI removal by PFl-1 was minimal. The higher apparent removal of AMI from solution at high solution pH was due to precipitation instead of adsorption. The fast uptake of AMI by PFl-1 with a moderate adsorption capacity limited by CEC and the linear correlation between AMI adsorption and cation desorption implied surface adsorption via a cation exchange mechanism at pH 6–7. The 10% smectite content had strong effect on the total CEC of PFl-1, and thus, the removal of AMI by PFl-1. Taking into account the effects of smectite, the AMI adsorption on the palygorskite alone could reach a capacity of 0.056 mmol g^{-1} with a fast adsorption rate and relatively strong interaction through a cation exchange mechanism on the external surface. The results indicated that palygorskite could be an effective adsorbent for the removal of cationic drugs of low concentrations in wastewater treatments.

Acknowledgments

The financial support from grants MOST 104-2811-M-006-001 and MOST104-2116-M-006-011 from the Ministry of Science and Technology, Taiwan is greatly appreciated.

References

Ahmet, R.M., Angel, F.C., 2001. Baseline studies of the Clay Minerals Society source clays: chemical analyses of major elements. Clays Clay Min. 49, 381–386.
Banu, S.U.N., Maheswaran, G., Ramesh, N., 2015. Modelling of equilibrium data for the adsorption of crystal violet onto activated carbon by non-linear regression method. Int. J. Innov. Res. Sci. Eng. Technol. 4, 15–22.
Bindya, S., Wong, W.T., Ashok, M.A., Yathirajan, H.S., Rathore, R.S., 2007. Amitriptylinium picrate: conformational disorder. Acta Crystallogr. C Cryst. Struct. Commun. 63, O546–O548.
Blanchard, G., Maunaye, M., Martin, G., 1984. Removal of heavy-metals from waters by means of natural zeolites. Water Res. 18, 1501–1507.
Blessel, K.W., Rudy, B.C., Senkowski, B.Z., 1974. Amitriptyline hydrochloride. Anal. Profiles Drug Subst. 3, 127–148.
Borden, D., Giese, R.F., 2001. Baseline studies of the Clay Minerals Society source clays: cation exchange capacity measurements by the ammonia-electrode method. Clays Clay Min. 49, 444–445.
Calisto, V., Esteves, V.I., 2009. Psychiatric pharmaceuticals in the environment. Chemosphere 77, 1257–1274.
Chang, P.-H., Jiang, W.-T., Li, Z., Kuo, C.-Y., Jean, J.-S., Chen, W.-R., Lv, G., 2014. Mechanism of amitriptyline adsorption on Ca-montmorillonite (SAz-2). J. Hazard. Mater 277, 44–52.
Chang, P.-H., Jiang, W.-T., Li, Z., Kuo, C.-Y., Wu, Q., Jean, J.-S., Lv, G., 2016. Interaction of ciprofloxacin and probe compounds with palygorskite. J. Hazard. Mater 303, 55–63.
Chang, P.-H., Li, Z., Yu, T.-L., Munkhbayer, S., Kuo, T.-H., Hung, Y.-C., Jean, J.-S., Lin, K.-H., 2009. Sorptive removal of tetracycline from water by palygorskite. J. Hazard. Mater 165, 148–155.

Chipera, S.J., Bish, D.L., 2001. Baseline studies of the Clay Minerals Society source clays: powder X-ray diffraction analyses. Clays Clay Min. 49, 398–409.
Dogan, A.U., Dogan, M., Onal, M., Sarikaya, Y., Aburub, A., Wurster, D.E., 2006. Baseline studies of the Clay Minerals Society source clays: specific surface area by the Brunauer Emmett Teller (BET) method. Clays Clay Min. 54, 62–66.
Galan, E., 1996. Properties and applications of palygorskite-sepiolite clays. Clay Min. 31, 443–454.
Gehring, A.U., Keller, P., Prey, B., Luster, J., 1995. The occurrence of spherical morphology as evidence for changing conditions during the genesis of a sepiolite deposit. Clay Min. 30, 83–86.
Green, A.L., 1967. Ionization constants and water solubilities of some aminoalkylphe-nothiazine tranquillizers and related compounds. J. Pharm. Pharmacol. 19, 10–16.
Heimstad, E., Edvardsen, Ø., Ferrin, T.E., Dahl, S.G., 1991. Molecular structure and dynamics of tricyclic antidepressant drugs. Eur. Neuropsychopharmacol. 1, 127–137.
Hörsing, M., Ledin, A., Grabic, R., Fick, J., Tysklind, M., la Cour Jansen, J., Andersen, H.R., 2011. Determination of sorption of seventy-five pharmaceuticals in sewage sludge. Water Res. 45, 4470–4482.
Hyland, K.C., Dickenson, E.R.V., Drewes, J.E., Higgins, C.P., 2012. Sorption of ionized and neutral emerging trace organic compounds onto activated sludge from different wastewater treatment configurations. Water Res. 46, 1958–1968.
Jaynes, W.F., Zartman, R.E., Green, C.J., San Francisco, M.J., Zak, J.C., 2005. Castor toxin adsorption to clay minerals. Clays Clay Min. 53, 268–277.
Kasprzyk-Hordern, B., Dinsdale, R.M., Guwy, A.J., 2009. The removal of pharmaceuticals, personal care products, endocrine disruptors and illicit drugs during wastewater treatment and its impact on the quality of receiving waters. Water Res. 43, 363–380.
Lamani, S.D., Nandibewoor, S.T., 2011. Oxidation of tricyclic antidepressant agent, amitriptyline, by permanganate in sulphuric acid medium: kinetic and mechanistic approach. J. Thermodyn. Catal. 2, 110. http://dx.doi.org/10.4172/2157-7544.1000110.
Ledesma, B., Román, S., González, J.F., Zamora, F., Rayo, M.C., 2010. Study of the mechanisms involved in the adsorption of amitriptyline from aqueous solution onto activated carbons. Adsorpt. Sci. Technol. 28, 739–750.
Lee, D.-W., Flint, J., Morey, T., Dennis, D., Partch, R., Baney, R., 2005. Aromatic-aromatic interaction of amitriptyline: implication of overdosed drug detoxification. J. Pharma. Sci. 94, 373–381.
Li, H., Sumarah, M.W., Topp, E., 2013. Persistence of the tricyclic antidepressant drugs amitriptyline and nortriptyline in agriculture soils. Environ. Toxicol. Chem. 32, 509–516.
Li, Z., Fitzgerald, N.M., Jiang, W.-T., Lv, G., 2016. Palygorskite for the uptake and removal of pharmaceuticals for wastewater treatment. Process Saf. Environ. Prot. http://dx.doi.org/10.1016/j.psep.2015.09.008 in press.
Lv, G., Stockwell, C., Niles, J., Minegar, S., Li, Z., Jiang, W.-T., 2013. Uptake and retention of amitriptyline by kaolinite. J. Colloid Interface Sci. 411, 198–203.
Madejova, J., Komadel, P., 2001. Baseline studies of the Clay Minerals Society source clays: infrared methods. Clays Clay Min. 49, 410–432.
Manzo, R.H., Olivera, M.E., Amidon, G.L., Shah, V.P., Dressman, J.B., Barends, D.M., 2006. Biowaiver monographs for immediate release solid oral dosage forms: amitriptyline hydrochloride. J. Pharm. Sci. 95, 966–973.
Murray, H.H., Pozo, M., Galán, E., 2011. An introduction to palygorskite and sepiolite deposits—Location, geology and uses. Dev. Clay Sci. 3, 85–99.
Nabais, J.M., Ledesma, B., Laginhas, C., 2012. Removal of amitriptyline from aqueous media using activated carbons. Adsorpt. Sci. Technol. 30, 255–263.
Richardson, M.L., Bowran, J.M., 1985. The fate of pharmaceutical chemicals in the aquatic environment. Pharm. Pharmacol. 37, 1–12.
Sanchez, A.G., Ayuso, E.A., De Blas, O.J., 1999. Sorption of heavy metals from industrial waste water by low-cost mineral silicates. Clay Min. 34, 469–477.
Sebastine, I.M., Wakeman, R.J., 2003. Consumption and environmental hazards of pharmaceutical substances in the Uk. Trans. IChemE 81, 229–235.
Shuali, U., Nir, S., Rytwo, G., 2011. Adsorption of surfactants, dyes and cationic herbicides on sepiolite and palygorskite: modifications, applications and modelling. In: Galan, E., Singer, A. (Eds.), Developments in Palygorskite-sepiolite Research: a New Outlook on These Nanomaterials. Elsevier, Oxford, U.K, pp. 351–374.
Stevens-Garmon, J., Drewes, J.E., Khan, S.J., McDonald, J.A., Dickenson, E.R.V., 2011. Sorption of emerging trace organic compounds onto wastewater sludge solids. Water Res. 45, 3417–3426.
Taboada, P., Ruso, J.M., Garcia, M., Mosquera, V., 2001. Surface properties of some amphiphilic antidepressant drugs. Colloids Surf. A Physicochem. Eng. Asp. 179, 125–128.
Tadkaew, N., Hai, F.I., McDonald, J.A., Khan, S.J., Nghiem, L.D., 2011. Removal of trace organics by MBR treatment: the role of molecular properties. Water Res. 45, 2439–2451.
Taha, D.N., Samaka, I.S., Mohammed, L.A., 2013. Adsorptive removal of dye from industrial effluents using natural Iraqi palygorskite clay as low-cost adsorbent. J. Asian Sci. Res. 3, 945–955.
Vijaya, R., Pratheeba, C., Anuzvi, A., Sanoj, V., Kumar, J., 2015. Study of the hydroxy propyl methyl cellulose (HPMC) combinations in the development of transdermal film for amitriptyline HCl and their in vitro characterization. Int. J. Pharm. Chem. Biol. Sci. 5, 548–556.